Development 135, 2815-2825 (2008) doi:10.1242/dev.020586

Tissue-specific requirements of β-catenin in external genitalia development

Congxing Lin[1,4], Yan Yin[1], Fanxin Long[2,3] and Liang Ma[1,2,*]

External genitalia are body appendages specialized for internal fertilization. Their development can be divided into two phases, an early androgen-independent phase and a late androgen-dependent sexual differentiation phase. In the early phase, the embryonic anlage of external genitalia, the genital tubercle (GT), is morphologically identical in both sexes. Although congenital external genitalia malformations represent the second most common birth defect in humans, the genetic pathways governing early external genitalia development and urethra formation are poorly understood. Proper development of the GT requires coordinated outgrowth of the mesodermally derived mesenchyme and extension of the endodermal urethra within an ectodermal epithelial capsule. Here, we demonstrate that β-catenin plays indispensable and distinct roles in each of the aforementioned three tissue layers in early androgen-independent GT development. WNT-β-catenin signaling is required in the endodermal urethra to activate and maintain *Fgf8* expression and direct GT outgrowth, as well as to maintain homeostasis of the urethra. Moreover, β-catenin is required in the mesenchyme to promote cell proliferation. By contrast, β-catenin is required in the ectoderm to maintain tissue integrity, possibly through cell-cell adhesion during GT outgrowth. The fact that both endodermal and ectodermal β-catenin knockout animals develop severe hypospadias in both sexes raises the possibility that the deregulation of any of these functions can contribute to the etiology of congenital external genital defects in humans.

KEY WORDS: β-Catenin, Genitalia, Urethra, *Fgf8*, Hypospadias

INTRODUCTION

External genitalia development starts at around 4 weeks of gestation in humans (Spaulding, 1921; Yamada et al., 2003) and on embryonic day 10.5 (E10.5) in mice (Perriton et al., 2002; Suzuki et al., 2002), when paired genital swellings form on either side of the cloaca. The swellings subsequently merge medially to form the genital tubercle (GT) and continue to grow distally. Within the GT, cloacal endoderm extends distally to form the future urethra (Felix, 1912; Kurzrock et al., 1999a; Perriton et al., 2002). Early GT development involves coordinated growth and patterning of cells from the ectodermally derived surface epithelium, the mesodermally derived mesenchyme and the endodermally derived urethral epithelium (UE) (Kurzrock et al., 1999a; Perriton et al., 2002). Up to E15.5, male and female GTs are morphologically indistinguishable (Suzuki et al., 2002), and their development is presumably controlled by the same genetic program. On and after E16.5, the urethrae in males canalize in the presence of androgen signaling, whereas they remain as an epithelial cord in females (Baskin et al., 2001; Suzuki et al., 2002; Yamada et al., 2003). We focused on studying the genetic program regulating early androgen-independent GT patterning.

Both the GT and the limb bud share similar morphogenetic and signaling pathways, perhaps reflecting a similar evolutionary origin (teleost fins). *Shh* (Haraguchi et al., 2001; Perriton et al., 2002), *Wnt5a* (Suzuki et al., 2003; Yamaguchi et al., 1999), *Bmp4*, *Bmpr1a* and noggin (Dunn et al., 1997; Suzuki et al., 2003), and HOX genes (*Hoxd13* and *Hoxa13*) (Dolle et al., 1993; Fromental-Ramain et al., 1996; Morgan et al., 2003; Warot et al., 1997; Zakany et al., 1997), are all essential for the development of both appendages. In addition, both processes require an epithelial signaling center marked by *Fgf8* expression, namely the distal urethral epithelium (dUE) in the GT (Cohn, 2004; Haraguchi et al., 2000; Suzuki et al., 2003; Yamada et al., 2006) and the apical ectodermal ridge (AER) in the limb (Cohn et al., 1995; Crossley et al., 1996; Lewandoski et al., 2000; Mariani and Martin, 2003; Niswander et al., 1993; Saunders, 1948; Summerbell, 1974). Several lines of evidence support the notion that FGF8 is the GT outgrowth-promoting factor. First, surgical removal of *Fgf8*-expressing dUE resulted in defective GT outgrowth. Second, neutralizing FGF8 with antibody caused similar outgrowth defects. Finally, outgrowth in dUE-deficient GTs can be restored by the application of FGF8 protein beads (Haraguchi et al., 2000). However, in contrast to the AER, little is known about how the dUE is established and maintained within the endodermal cloaca, and how it functions to promote GT outgrowth. The development of the GT differs from that of the limb bud in that GT growth and patterning has to be coordinated with endodermal urethral development, which requires *Fgf10*/*Fgfr2* signaling (Petiot et al., 2005) and *Hoxa13* (Morgan et al., 2003; Scott et al., 2005). Last, but not least, the GT forms with left-right symmetry, whereas the limb develops asymmetrically. Although both *Wnt5a*$^{-/-}$ and *Tcf1*/*Tcf4* double-knockout embryos show GT agenesis (Gregorieff et al., 2004; Suzuki et al., 2003; Yamaguchi et al., 1999), both mutants exhibit severe caudal truncations, raising the concern that the genital phenotype in these mutants might be secondary. Therefore, the involvement of WNT signaling in GT development is not clear. In this study, by using tissue-specific inactivation of β-catenin, a key signal transducer of the canonical WNT pathway, we show that β-catenin-mediated WNT signaling is required at multiple stages for directing GT outgrowth and urethra formation. β-Catenin function is also required in the ventral ectoderm to maintain epithelial integrity.

[1]Division of Dermatology, [2]Department of Developmental Biology, and [3]Division of Bone and Mineral Diseases, Department of Medicine, Washington University School of Medicine, 660 S. Euclid Avenue, St. Louis, MO 63110, USA. [4]Human Genetics Program, Tulane University School of Medicine, New Orleans, LA 70112, USA.

*Author for correspondence (e-mail: lima@dom.wustl.edu)

Accepted 13 June 2008

MATERIALS AND METHODS

Animal maintenance and treatment

Msx2-Cre, *Shh*$^{Cre/GFP}$, *Shh*$^{tm(Cre/Esr1)}$, TOPGAL and R26R strains were purchased from the Jackson Laboratory (Bar Harbor, MN). *Shh*$^{Cre/GFP}$ and *Shh*$^{tm(Cre/Esr1)}$ transgenic lines express an EGFP-Cre fusion protein and a tamoxifen-inducible Cre from the endogenous *Shh* locus, respectively (Harfe et al., 2004). *β-Cat*$^{flox/flox}$ (LOF), *β-Cat*$^{loxEx3/loxEx3}$ (GOF) and *Dermo1-Cre* strains were described previously (Brault et al., 2001; Harada et al., 1999; Yu et al., 2003). Briefly, *β-Cat*$^{flox/flox}$ mice bear two LoxP sites flanking exons 2-6, which will lead to a loss-of-function deletion upon Cre-mediated excision. *β-Cat*$^{loxEx3/loxEx3}$ mice have only exon 3 floxed, deletion of which leads to a stabilized form of β-catenin. Tamoxifen (Sigma-Aldrich, St Louis, MO) was dissolved in corn oil at a concentration of 20 mg/ml and was delivered by gavaging pregnant females at a dose of 0.2 g/kg of body weight. For studies involving embryos from E14.5 onward, only males were presented (except for the study shown in Fig. S5D in the supplementary material).

In situ hybridization

^{35}S in situ hybridizations were performed on paraformaldehyde (PFA)-fixed, paraffin-embedded, 10-μm sections, as described previously (Wawersik and Epstein, 2000). Whole-mount in situ hybridization was performed as previously described (Wilkinson, 1992). Probes for *Tcf1*, *Lef1*, *Tcf4* and *Ptc1* (Hu et al., 2005), *Shh* (Bitgood and McMahon, 1995), *Msx2* (Yin et al., 2006), *Wnt5a* (Huang et al., 2005), *Hoxa13* and *Hoxd13*, *Bmp4* (Jones et al., 1991) and *Fgf8* (Crossley and Martin, 1995) were described previously. The *Wnt11* probe was a gift from Dr Andy McMahon (Harvard University, Cambridge, MA). *Wnt9b*, *Wnt2* and *Wnt3* probes were generated using ATCC clones or PCR amplification.

Histology and immunofluorescence

Embryos were fixed in Bouin's fixative, embedded in paraffin after dehydration and sectioned at 5 μm. Hematoxylin and eosin staining and X-gal analyses were performed following standard protocols. Immunofluorescence was performed as described previously (Yin et al., 2006). Primary antibodies used in this study (all in 1:300 dilutions) were as follows: anti-β-catenin, anti-E-cadherin, anti-plakoglobin (BD biosciences, San Jose, CA), and anti-phosphoH3 (Millipore, Billeric, MA).

Electron microscopy analysis

For scanning electron microscopy (SEM) analysis, samples were fixed in 3% glutaraldehyde, post-fixed with 1% aqueous osmium tetroxide for 4 hours, then processed using the Osmium-Thiocarbohydrazide-Osmium (OTO) method, dehydrated in alcohol and critical-point dried in liquid CO_2. Mounted samples were sputter-coated and examined in a Hitachi S-450 SEM. For transmission electron microscopy (TEM) and semi-thin histology, samples were fixed in paraformaldehyde and glutaraldehyde, and post-fixed with aqueous 1% OsO_4 for 2 hours. Samples were dehydrated, subjected to three changes of propylene oxide, and infiltrated with Polybed 812 epoxy embedding resin. Specimen blocks were polymerized at 60°C in a vacuum oven. Thin sections were generated, post-stained with 2.5% uranyl acetate and lead citrate, and examined in a Hitachi H-600 TEM, or post-stained with Epoxy Tissue Stain (catalogue number 14950, Electron Microscopy Sciences, Hatfield, PA) and followed by light microscopy.

Apoptosis assay

TUNEL staining was performed on PFA-fixed, paraffin-embedded, 10-μm sections using the In Situ Cell Death Kit (Roche Diagnostic, Indianapolis, IN), according to the manufacturer's instructions.

Statistics

Data were analyzed by unpaired Student's *t*-test, and results are expressed as means±s.e.m. The number of independent experiments is specified in the Results.

RESULTS

WNT activities during early GT development

To determine whether canonical WNT signaling is activated in the developing mouse GT, we used TOPGAL transgenic mice to report canonical WNT-β-catenin activity (DasGupta and Fuchs, 1999). In the cloaca region, transgene activity was first detected at E10.5 (Fig. 1A). Sections of stained embryos revealed that β-galactosidase (β-gal)-positive cells were localized to the cloacal endoderm (Fig. 1E, arrows). As GT development progressed, this distal urethral β-gal expression persisted (Fig. 1B-F, arrows). Distinct populations of β-gal-positive cells were also detected on the proximolateral sides of the GT at E13.5 (Fig. 1C, arrowheads) and in the labioscrotal swellings at E14.5 (Fig. 1D, arrowheads). Next, we examined the expression of transcriptional mediators of WNT signaling, T-cell factors, in the GT. RT-PCR analysis showed that *Tcf1* (*Tcf7* – Mouse Genome Informatics), *Lef1* and *Tcf4* (*Tcf7l2* – Mouse Genome Informatics) were expressed throughout GT development (see Table S1 in the supplementary material), and ^{35}S-in situ hybridization revealed that *Tcf1* and *Tcf4* were co-expressed in the dUE where TOPGAL activity was detected (Fig. 1G,H, arrows). In addition, *Tcf1* transcripts were also detected in the ventral ectoderm and distal mesenchyme, while *Tcf4* was also expressed in the proximal UE (Fig. 1G,H, arrowheads). By contrast, *Lef1* was only expressed in distal GT mesenchyme (see Fig. S1F in the supplementary material). To identify WNT ligands that may activate canonical WNT signaling in the GT, we performed RT-PCR using RNA extracted from E11.5, E12.5 and E14.5 GTs and ^{35}S-in situ hybridization in E12.5 GTs. Several WNT ligands, including *Wnt2*, *Wnt3*, *Wnt4*, *Wnt5a*, *Wnt9b* and *Wnt11* were expressed in the developing GT, with *Wnt5*a and *Wnt9b* expression detected in the dUE (see Table S1 and Fig. S1A-E in the supplementary material). Together, these data demonstrate that WNT signaling is activated during GT development.

Initiation of *Fgf8* expression by WNT-β-catenin signaling

To analyze the function of β-catenin in all three tissue layers during GT development, we used transgenic Cre lines to either conditionally remove or activate β-catenin. We first analyzed tissue specificity of the Cre lines by crossing them with *Rosa26-lacZ* reporter mice (*R26R*) (Soriano, 1999). At E10.5, *Shh*$^{cre/Gfp}$;*R26R* embryos showed Cre-mediated recombination exclusively in the cloacal endoderm (Fig. 1J), whereas *Msx2-Cre* and *Dermo1-Cre* lines conferred Cre activity in the ectodermal epithelium and mesodermal mesenchyme, respectively (Fig. 1K,L). The tissue-specific Cre expression in all three lines persisted throughout early GT development (data not shown).

As strong TOPGAL activity was detected in the dUE, we first examined the function of β-catenin in GT endoderm. *Shh*$^{cre/Gfp}$ mice were crossed to either *β-Cat*$^{c/c}$ (Brault et al., 2001) or *β-Cat*^{loxEx3} (Harada et al., 1999) mice to generate endodermal loss- or gain-of-function (LOF or GOF) embryos. At E10.5, no morphological difference in the cloaca region was observed between wild-type and LOF embryos. At E12.5, scanning electron microscopy (SEM) revealed a cone-shaped GT with a centered urethral seam on the ventral side in wild-type embryos (Fig. 2A). By contrast, *Shh*$^{cre/Gfp}$*;β-cat*$^{c/c}$ (LOF) embryos exhibited a severe outgrowth defect, in which GT failed to form and, instead, a crater-like structure was present (Fig. 2B). Both male and female mutants were equally affected. At E18.5, only a small remnant was detected in the presumptive genital region (data not shown). Immunofluorescence confirmed the complete removal of β-catenin protein from the dUE (Fig. 2E). Because β-catenin is required in the limb ectoderm to establish the AER and to regulate *Fgf8* expression (Barrow et al., 2003), we reasoned that a similar mechanism might also apply to GT development. This hypothesis was supported by the colocalization of TOPGAL activity with *Fgf8* expression in wild-type dUE at both

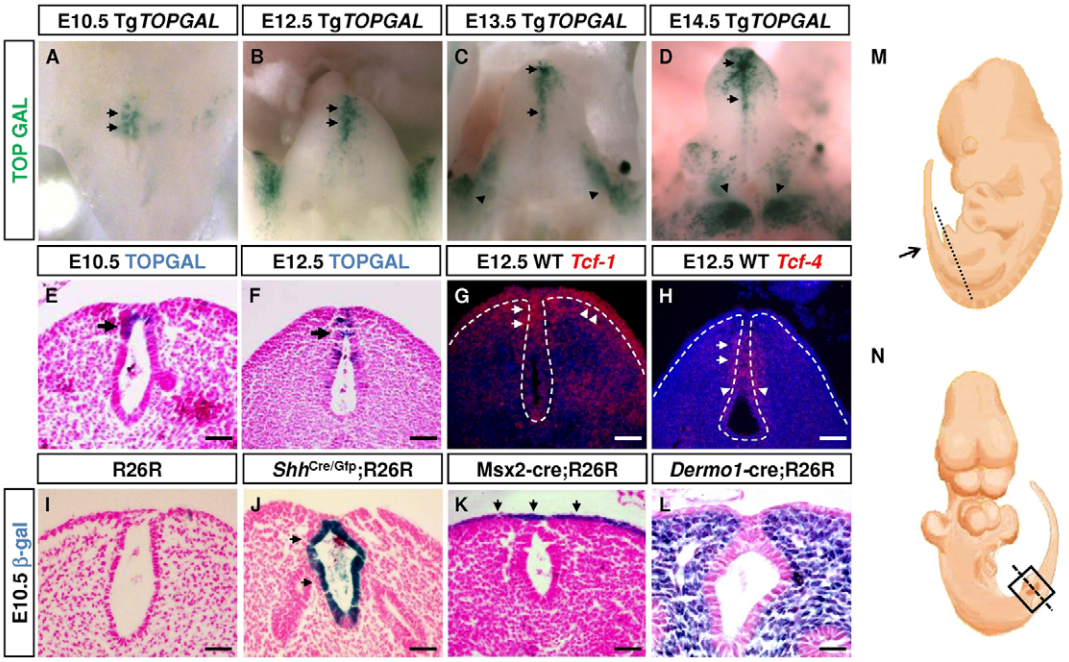

Fig. 1. WNT signaling in the developing GT and tissue-specific Cre expression. (**A-D**) TOPGAL embryos stained with X-Gal at different stages. TOPGAL expression in the dUE persists from E10.5 to E14.5 (arrows, A-D). Preputial swellings (arrowheads, C) and labioscrotal swellings (arrowheads, D) are also positive for TOPGAL activity. (**E**,**F**) Coronal sections of E10.5 and E12.5 GTs showing distal urethral localization of TOPGAL positive cells (blue). (**G**,**H**) ^{35}S in situ hybridization on E12.5 GT sections (plane of section is shown in M) using probes indicated. (**I-L**) Coronal sections (plane of section is shown in N) of X-Gal-stained E10.5 embryos showing tissue-specific Cre-mediated recombination in the GTs. No endogenous X-Gal activity was detected at this stage (I). Scale bars: 100 μm in F-H; 50 μm in E,I-L.

E10.5 and E12.5 (see Fig. S2A-D in the supplementary material). Consistent with this hypothesis, *Fgf8* was never detected in the distal cloacal endoderm of *Shh*$^{cre/Gfp}$;*β-cat*$^{c/c}$ embryos from E10.5 onwards (Fig. 2H, data not shown). Consequently, expression of *Bmp4*, a downstream target of *Fgf8* (Haraguchi et al., 2000), was markedly reduced in mutant GT mesenchyme (Fig. 2K). Previous reports demonstrated that disrupting AER by either physical or genetic means caused increased cell death and decreased cellular proliferation (Barrow et al., 2003; Dudley et al., 2002). Similarly, increased apoptosis in both endoderm and mesenchyme of E10.5 *Shh*$^{cre/Gfp}$;*β-Cat*$^{c/c}$ GTs (Fig. 2M,N,O; 2.48±0.6% in controls versus 10.9±2.49% in mutants, n=10, P<0.0001) was revealed by TUNEL assay. We also detected a decrease in cell proliferation, evidenced by a twofold reduction in phospho histone-H3 (PHH3)-positive cells in E10.5 mutant endoderm (Fig. 2P,Q,R; 6.84±0.99% in controls versus 3.03±0.6% in mutants, n=10, P<0.0001). By contrast, *Hoxa13* and *Fgf10* were properly expressed in the LOF mutants, which provides evidence against a global gene expression change as a result of reduced cell numbers (data not shown). Altogether, the loss of *Fgf8* induction, the increased cell death and the decreased proliferation are all consistent with a failure of dUE establishment in the LOF mutant embryos, indicating an obligatory role for WNT-β-catenin in establishing the GT signaling center.

To further examine the role of WNT signaling in dUE establishment, we analyzed GT development in endodermal GOF embryos. GTs of *Shh*$^{cre/Gfp}$;*β-cat*^{loxEx3} embryos were much larger than those of wild types at E12.5, and immunostaining showed accumulation of β-catenin in the UE (Fig. 2C,F). In situ hybridization revealed that *Fgf8* was overexpressed in the GOF cloacal endoderm at E10.5 (Fig. 2I). Combined with LOF studies, these results clearly demonstrate that during GT initiation, WNT-β-catenin signaling is both necessary and sufficient to activate *Fgf8* expression in the endodermal cloaca. To test whether this genetic regulation between WNT-β-catenin and *Fgf8* is conserved in the limb bud, we generated limb ectodermal β-catenin GOF embryos by crossing *Msx2-Cre* with *β-Cat*^{loxEx3} mice. At E10.5, R26R reporter assays showed sporadic Cre activity in the inter-limb ectoderm in addition to in the dorsal and ventral ectoderm and the AER of the limb bud, as previously reported (Barrow et al., 2003) (Fig. 2V). Intriguingly, ectopic *Fgf8* expression was detected in similar sporadic areas in the inter-limb ectoderm of *Msx2-Cre*;*β-Cat*^{loxEx3} embryos (Fig. 2U), likely corresponding to Cre-mediated β-catenin activation in those cells. Furthermore, ectopic outgrowth was observed in the inter-limb ectoderm of *Msx2-Cre*;*β-Cat*^{loxEx3} embryos at E12.5 (Fig. 2X, arrows). These results indicate that activation of *Fgf8* by WNT-β-catenin signaling is conserved between the limb ectoderm and dUE, and that this genetic regulation is essential for directing appendage outgrowth.

Requirement of WNT-β-catenin during GT outgrowth and urethra development

The early phenotype in *Shh*$^{cre/Gfp}$;*β-Cat*$^{c/c}$ mice prevented us from studying the function of β-catenin during GT outgrowth and urethra formation. To circumvent this limitation, we employed a tamoxifen (Tm)-inducible *Shh*$^{Cre/esr}$ line (Harfe et al., 2004). In this experiment, Cre-mediated recombination can be detected as early as 12 hours after Tm treatment and robust recombination was evident in the UE 24 hours after Tm treatment (data not shown). We generated *Shh*$^{Cre/esr}$;*β-Cat*$^{c/c}$ and *Shh*$^{Cre/esr}$;*β-Cat*^{loxEx3} embryos for LOF and GOF studies, respectively. Cre activity was induced at E9.5, E10.5

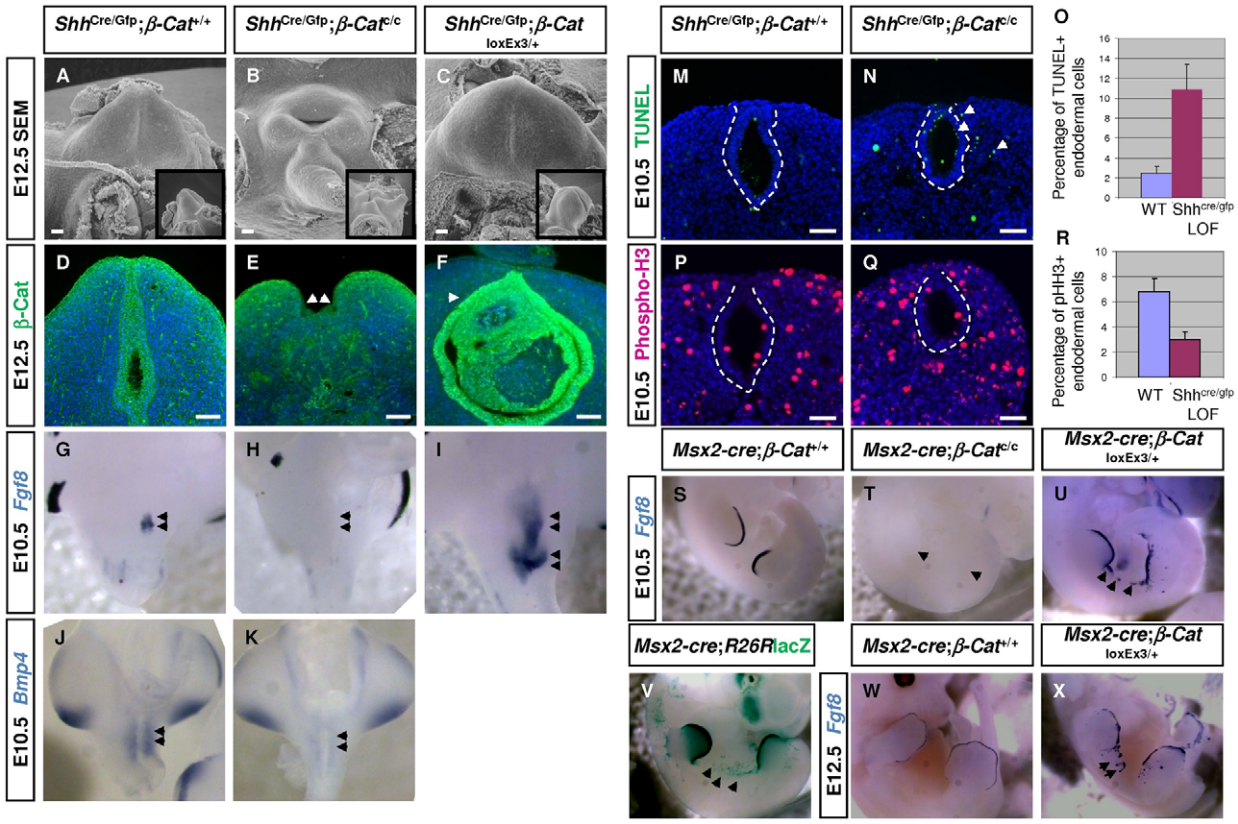

Fig. 2. Endodermal WNT-β-catenin signaling is required for GT initiation. (**A-C**) SEM analysis showing an absence of GT outgrowth in the *Shh*$^{cre/Gfp}$;*β-Cat*$^{c/c}$ embryo (B) and a larger GT in the *Shh*$^{cre/Gfp}$;*β-Cat*^{loxEx3} embryo (C). (**D-F**) β-Catenin indirect immunoflouresence showing that the protein was detected mainly on the cell membranes of both GT ectoderm and UE, as well as weakly in the mesechyme (D). Complete removal of β-catenin in the UE was confirmed in *Shh*$^{cre/Gfp}$;*β-Cat*$^{c/c}$ GT (arrows, E), and ectopic accumulation of β-catenin was observed in *Shh*$^{cre/Gfp}$;*β-Cat*^{loxEx3} endoderm (arrow, F). (**G-I**) Whole-mount *Fgf8* in situ hybridization showing expression in the distal cloacal endoderm in control embryos (G), but not in *Shh*$^{cre/Gfp}$;*β-Cat*$^{c/c}$ embryos (arrows, H); in *Shh*$^{cre/Gfp}$;*β-Cat*^{loxEx3} GT, *Fgf8* expression is ectopically expanded (I). (**J**,**K**) Whole-mount *Bmp4* in situ hybridization showing a reduction in *Shh*$^{cre/Gfp}$;*β-Cat*$^{c/c}$ cloacal mesenchyme (K). (**M-O**) TUNEL analysis showing increased cell death in *Shh*$^{cre/Gfp}$;*β-Cat*$^{c/c}$ cloacal endoderm and ectopic apoptotic cells in the surrounding mesenchyme (arrows in N). (**P-R**) PHH3 immunostaining revealing markedly reduced cell proliferation in E10.5 *Shh*$^{cre/Gfp}$;*β-Cat*$^{c/c}$ cloacal endoderm. (**S-U**,**W**,**X**) *Fgf8* in situ hybridization showing an absence of expression in E10.5 *Msx2-Cre*;*β-Cat*$^{c/c}$ limbs (T) and ectopic expression in the flank ectoderm and dorsal limb ectoderm in *Msx2*-cre;*β-Cat*^{loxEx3} embryos (U). (**V**) Note that ectopic *Fgf8* expression appears to correspond to *Msx2-Cre* expression (arrows in U,V). At E12.5, ectopic outgrowth was observed in the inter-limb region of *Msx2-Cre*;*β-Cat*^{loxEx3} embryos (arrows, X). Scale bars: 100 μm in A-F; 50 μm in M,N,P,Q.

or E11.5 for LOF studies and at E10.5 for GOF studies. Embryos were collected at E12.5 for molecular analysis and at E14.5 for histological analysis. To confirm that WNT-β-catenin signaling was perturbed in the mutants, we examined the expression of *Tcf1*, which is a transcriptional target of WNT signaling (Tu et al., 2007). As expected, *Tcf1* expression was markedly reduced in the LOF dUE (Fig. 3F′) and was activated in the entire UE of GOF GT at E12.5 (Fig. 3F″). At E14.5, SEM revealed that *Shh*$^{Cre/esr}$;*β-Cat*$^{c/c}$ GTs showed phenotypes with graded severity correlated with the timing of Cre induction (Fig. 3A-D). Specifically, earlier Tm treatments led to reduced distal growth (Fig. 3B-D, arrows) and larger proximal openings (Fig. 3B-D, arrowheads). By contrast, *Shh*$^{Cre/esr}$;*β-Cat*^{loxEx3} GT displayed excessive distal growth (Fig. 3E, arrow) with no proximal urethral opening (Fig. 3E, arrowhead). These phenotypes suggest a role for β-catenin in both GT outgrowth and urethra formation.

To test whether the reduced distal growth in LOF GTs resulted from decreased FGF8 signaling, we examined *Fgf8* expression in E12.5 *Shh*$^{Cre/esr}$;*β-Cat*$^{c/c}$ mutants treated with Tm at different times. *Fgf8* expression in the dUE was moderately reduced in E11.5-treated LOF embryos, dramatically reduced in E10.5-treated LOF embryos and completely absent in E9.5-treated LOF embryos (Fig. 3B′-D′). These results therefore indicate that the defective outgrowth in these LOF mutants is associated with altered FGF8 signaling. Thus, in addition to its function in *Fgf8* induction, WNT-β-catenin signaling is also required to maintain *Fgf8* expression during GT outgrowth. To investigate the function of endodermal WNT-β-catenin signaling in regulating mesenchymal gene expression, we examined the expression of mesenchymal genes in E10.5 Tm-treated wild-type and LOF embryos. Strong expression of *Msx2*, *Lef1* and *Wnt5a* was detected in the distal mesenchyme surrounding the wild-type dUE (Fig. 3H-J), but their expression domains were reduced in LOF GTs (Fig. 3H′-J′). By contrast, in the GOF GT, *Fgf8* expression was not only elevated in the distal UE but also ectopically induced in the proximal UE, indicating that at this stage ectopic WNT-β-catenin signaling can still activate *Fgf8* expression in UE (Fig. 3E′). Consistently, *Msx2*, *Lef1* and *Wnt5a* expression were ectopically expanded to more proximal mesenchyme (Fig. 3H″-J″). By contrast, contrary to previous results from an ex vivo study (Haraguchi et al., 2000), *Hoxa13* and *Hoxd13*

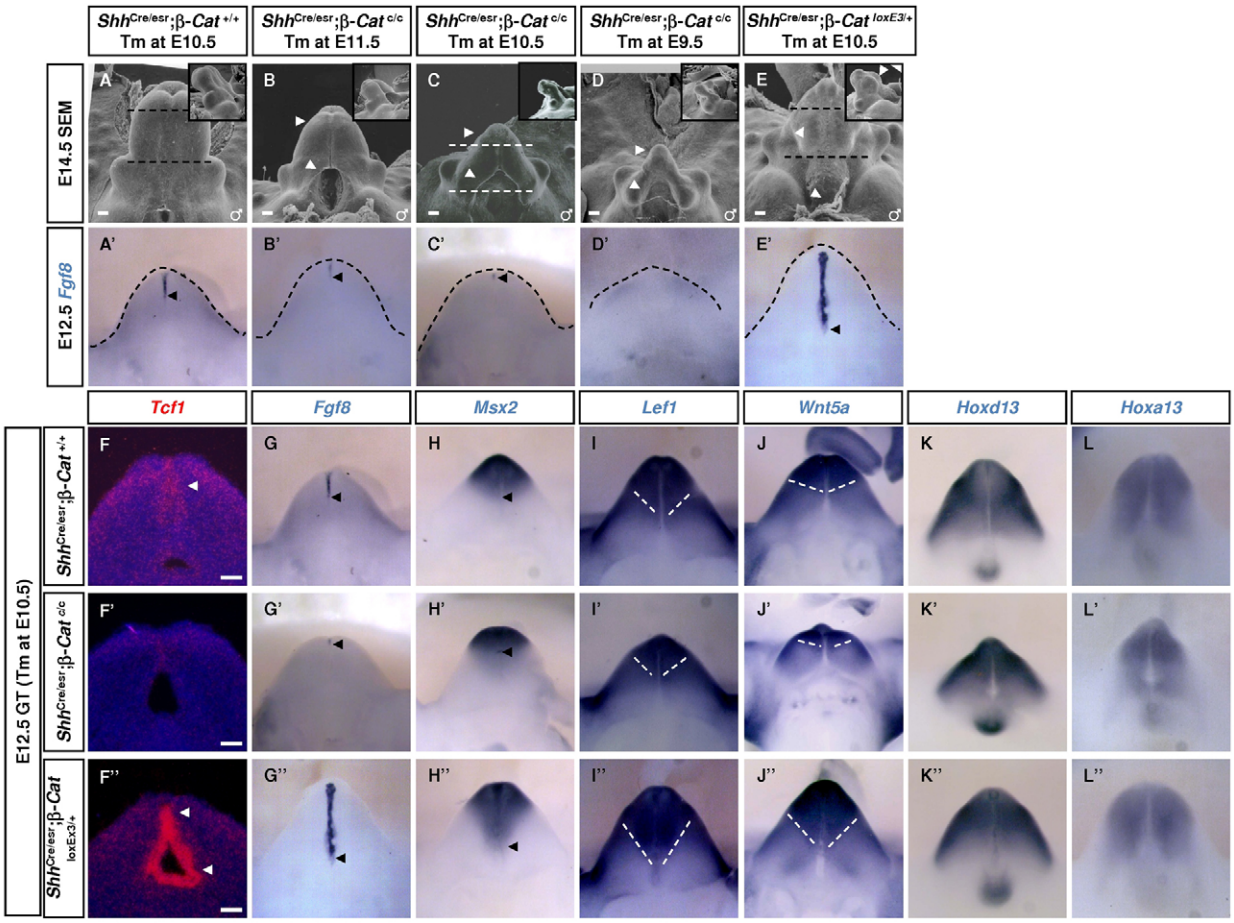

Fig. 3. Endodermal β-catenin is required to maintain GT outgrowth. (**A-E**) SEM analysis showing reduced distal growth and ectopic proximal opening in *Shh*$^{Cre/esr}$;β-Cat$^{c/c}$ embryos (arrowheads in B-D), and excessive distal growth with no proximal opening in *Shh*$^{Cre/esr}$;*β-Cat*^{loxEx3} GT (arrowheads, E). Dashed lines in A, C and E indicate the plane of transverse sections used for histological/immunostaining analysis in Fig. 4. (**A′-E′**) *Fgf8* in situ hybridization on E12.5 GTs. Note the graded decrease in *Fgf8* in LOF GTs (B′-D′). *Fgf8* is both elevated and ectopically activated in GOF GT (E′). (**F-F″**) ^{35}S *Tcf-1* in situ hybridization revealed downregulation of *Tcf1* in *Shh*$^{Cre/esr}$;*β-cat*$^{c/c}$ dUE (F′), and upregulation and ectopic proximal UE expression in *Shh*$^{Cre/esr}$;*β-Cat*^{loxEx3} GT (F″). (**G-L″**) Whole-mount in situ analysis using the probes indicated. *Msx2* is expressed in the distal mesenchyme surrounding the dUE (H). Its expression domain is reduced in *Shh*$^{Cre/esr}$;*β-Cat*$^{c/c}$ (H′), and is expanded proximally in *Shh*$^{Cre/esr}$;*β-Cat*^{loxEx3} GT (H″). *Lef1* and *Wnt5a* are strongly expressed in the distal mesenchyme, and this strong-expressing domain is also reduced in *Shh*$^{Cre/esr}$;*β-Cat*$^{c/c}$ GT (I′,J′), and expanded proximally in *Shh*$^{Cre/esr}$;*β-Cat*^{loxEx3} GT (I″,J″). *Hoxa13* and *Hoxd13* expression remains unchanged in either mutant (K-K″ and L-L″, respectively). Scale bars: 100 μm in A-E; 100 μm in F-F″.

were not significantly altered, despite dramatic changes in *Fgf8* expression (Fig. 3K-L″). Thus, endodermal WNT-β-catenin signaling controls the expression of *Msx2*, *Lef1* and *Wnt5a* in the distal mesenchyme but not expression of the HOX genes.

Next, we examined urethra formation in LOF mutants. In E14.5 wild-type GTs, endodermal cells formed a solid urethral plate in the distal region (Fig. 4A,A′) and a urethral tube at the proximal end (Fig. 4D,D′). In LOF embryos, the distal urethral plate failed to form with endodermal cells displaying a tube-like structure (Fig. 4B,B′), while the proximal urethra was open (Fig. 4E,E′). This phenotype may result from either defective epithelial differentiation or a reduction in cell proliferation. We first assessed epithelial differentiation by examining the expression of K14 and p63, markers for progenitor cells in stratified epithelium. The expression of both markers was maintained in the urethra, suggesting the progenitor cells are still present in the mutant (Fig. 4B‴,E‴, data not shown). By contrast, PHH3 immunostaining at E12.5 showed reduced proliferation in *Shh*$^{Cre/esr}$;*β-Cat*$^{c/c}$ urethra (Fig. 5A′; 6.14±1.03% in controls versus 2.08±0.5% in mutants, n=10, P<0.001). We did not observe any change in apoptosis in the UE (see Fig. S3D′ in the supplementary material). The lack of cellular proliferation in the LOF urethra could result from the loss of *Shh* and/or *Fgf8* signaling, because these genes have been directly associated with proliferation in the GT (Haraguchi et al., 2001; Haraguchi et al., 2000; Suzuki et al., 2003). Consistently, both *Fgf8* (Fig. 3G′) and *Shh* were markedly downregulated in the mutant urethra (Fig. 5B′, see also Fig. S3A′ in the supplementary material). As expected, *Ptch1*, a transcriptional target of HH signaling was also reduced in the mesenchyme (Fig. S3B′ in the supplementary material). These results indicate that WNT-β-catenin signaling is required to maintain FGF8 and SHH signaling during urethra formation and to promote cell proliferation, but is not required for maintaining the progenitor cell population.

Shh$^{Cre/esr}$;*β-Cat*^{loxEx3} (GOF) GT, however, exhibited a disorganized urethral plate in the distal region (Fig. 4C,C′) and severe excessive endodermal growth confined to the proximal end

(Fig. 4F,F′). This region-specific phenotype correlated with an increase in PHH3 staining specifically at the proximal end (Fig. 5A″). The molecular basis for the differential response in proliferation between the distal and proximal endoderm is not clear. However, we noted that *Shh* was downregulated in the distal but not the proximal UE (Fig. 5B″, see also Fig. S3A″, arrows and arrowheads, respectively). Correspondingly, *Ptch1* was reduced in the distal but not the proximal mesenchyme (see Fig. S3B″, arrows and arrowheads). In addition, we found that *Bmp4* was ectopically expressed in the distal UE of $Shh^{Cre/esr}$;β-Cat^{loxEx3} embryos where *Shh* expression was reduced (compare Fig. 5B″,C″, arrows and arrowheads). Intriguingly, this ectopic *Bmp4* activation in the distal UE appeared to require WNT-β-catenin signaling, because it was not observed in LOF urethra where *Shh* was also repressed (Fig. 5C′). Consistent with *Bmp4* expression, phosphorylated-Smad1/5/8 was strongly upregulated in the GOF UE (see Fig. S3C″ in the supplementary material), but was reduced in LOF GT (Fig. S3C′). The different response to ectopic WNT signaling probably reflects intrinsic differences in gene regulation between the distal and proximal regions of the urethral epithelium.

Notably, both male and female endodermal mutants (both LOF and GOF) were equally affected. They either do not reach the stage of sexual differentiation ($shh^{Cre/esr}$ lines) or have an early developmental arrest in GT morphogenesis that does not allow normal sexual differentiation to occur ($Shh^{Cre/gfp}$ lines). Thus, these phenotypes reflect a requirement of β-catenin during the androgen-independent phase of GT development.

Function of ectodermal β-catenin in GT development

To examine the role of ectodermal β-catenin in GT development, we removed β-catenin from the ventral ectoderm using *Msx2-Cre*. *Msx2-Cre;β-Cat$^{c/c}$* embryos exhibited a severe GT phenotype. SEM showed that, at E12.5, the urethral seam was evident in wild-type GTs (Fig. 6A, arrows), but was not present in *Msx2-Cre;β-Cat$^{c/c}$* GTs (Fig. 6B). Mutant GTs developed a large proximal opening at E13.5, and distal GT bifurcated at E14.5 (arrowheads in Fig. 6D,F). At E16.5, mutant GTs were severely dysmorphic and preputial swellings failed to join on the ventral side (Fig. 6H, arrowhead). On E18, urethrae in wild-type males were canalized but they remained as an epithelial cord in females. By contrast, both mutant males and females showed complete open urethrae, evidenced by positive β-catenin staining in the outer-most epithelial lining (Fig. S6G,H, arrows, in the supplementary material). Thus, the phenotype reflected a role for ectodermal β-catenin during early GT patterning, but not a disrupted androgen response. To track the fate of ectodermal cells in the mutant GT, we performed lineage-tracing experiments by using the R26R reporter allele in combination with *Msx2-Cre*. In wild-type embryos, the ectodermally derived surface epithelium of the *Msx2-Cre* lineage covered the entire GT, except for a small proximal opening from E12.5 to E16.5 (Fig. 6I,K,M,O). By contrast, mutant ectoderm was disrupted at the ventral midline as early as E12.5, evidenced by an unstained region (Fig. 6J, arrowheads) that continued to expand as the GT grew (Fig. 6L,N,P). At E16.5, the entire ventral side of the mutant GT was devoid of

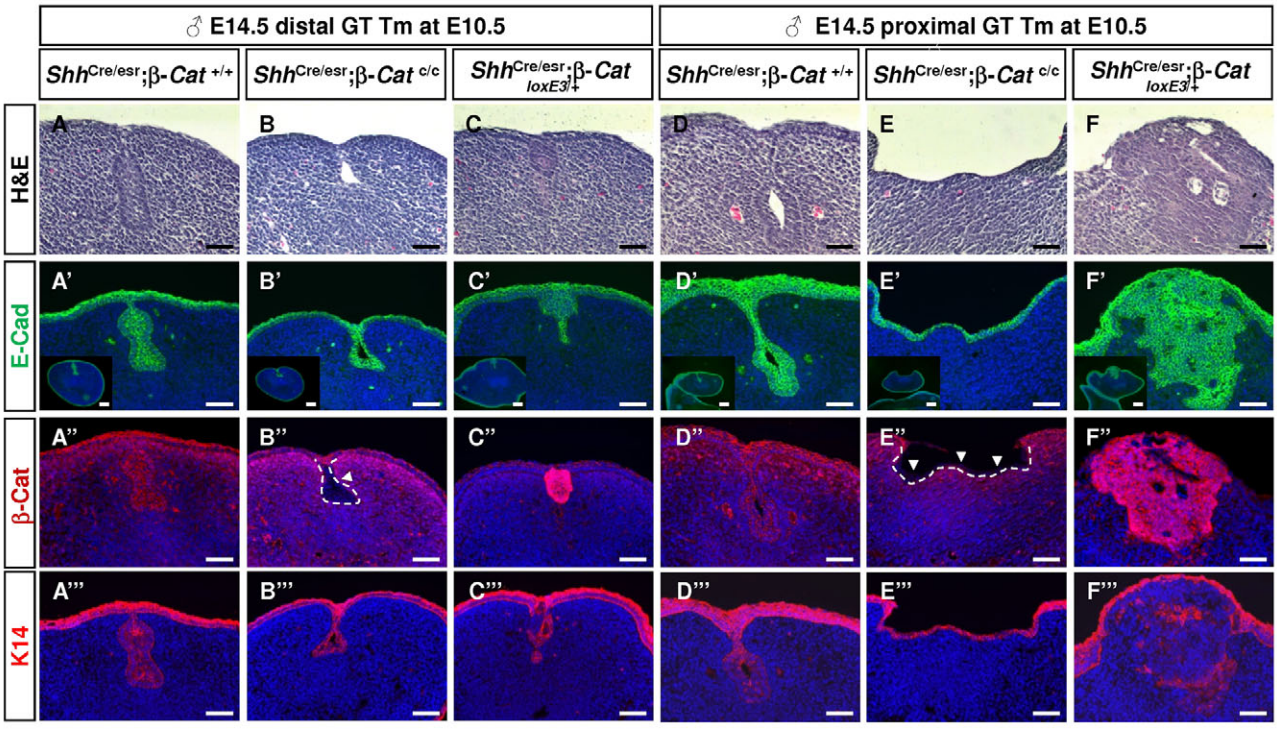

Fig. 4. Urethral defects in endodermal β-catenin LOF and GOF mutants. (**A-F′**) Hematoxylin and Eosin (H&E) staining (A-F) and indirect immunoflouresence for E-cadherin (A′-F′) on distal and proximal GTs. Note that in wild-type GT urethral cells form well-organized urethral plate distally (A,A′) but remain as a tube at the proximal end (D,D′). In $Shh^{Cre/esr}$;β-$Cat^{c/c}$ GT, urethral plate fails to form distally (B,B′), and the proximal urethra is open (E,E′). In $Shh^{Cre/esr}$;β-Cat^{loxEx3} GT, disorganized distal urethral plate is formed (C,C′), and the proximal urethra showed severe endodermal overgrowth (F,F′). (**A″-F″**) Immunostaining confirms that β-catenin protein is removed from $Shh^{Cre/esr}$;β-$Cat^{c/c}$ UE (arrowheads, B″,E″) and accumulates in $Shh^{Cre/esr}$;β-Cat^{loxEx3} UE (C″,F″). (**A‴-F‴**) Immunostaining showing K14 expression was detected in both surface epithelium and UE in wild-type GTs (A‴,D‴). The expression is maintained in LOF urethra (B‴,E‴) but is repressed in cells with high β-catenin expression in GOF urethra (C‴,F‴). Scale bars: 100 μm; 200 μm in insets.

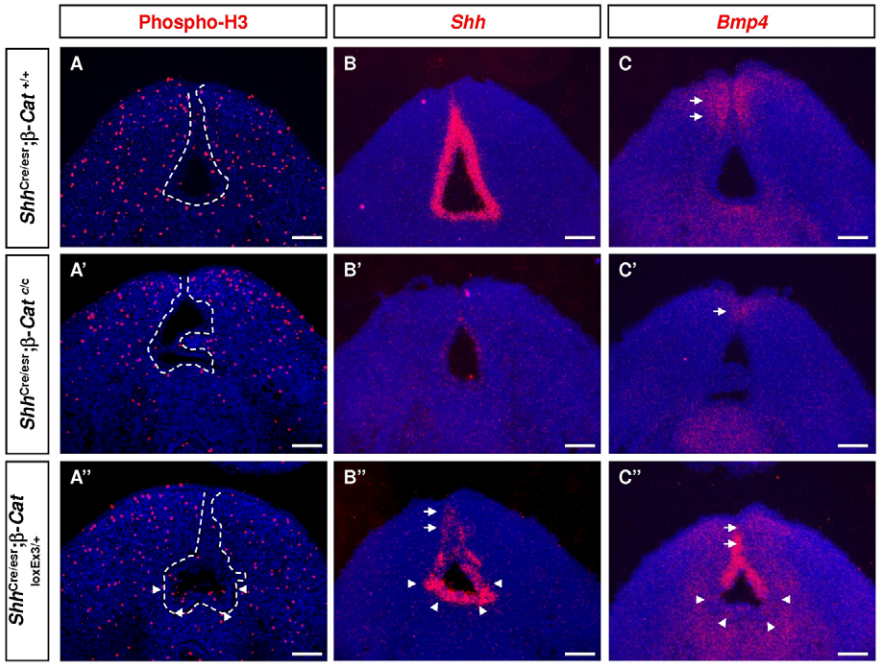

Fig. 5. Altered cellular proliferation and gene expression in endodermal β-catenin LOF and GOF urethrae. All embryos were exposed to Tm on E10.5 and collected on E12.5. (**A-A″**) PHH3 staining showed reduced cell proliferation in *Shh*$^{Cre/esr}$;*β-Cat*$^{c/c}$ UE (A′), and increased cell proliferation in proximal *Shh*$^{Cre/esr}$;*β-Cat*^{loxEx3} UE (arrowheads, A″). UE is highlighted by white dashed lines. (**B-C″**) ^{35}S in situ hybridization on adjacent coronal sections. *Shh* expression is downregulated in both *Shh*$^{Cre/esr}$;*β-Cat*$^{c/c}$ UE (B′) and distal *Shh*$^{Cre/esr}$;*β-Cat*^{loxEx3} UE (arrows, B″), but is maintained in the proximal *Shh*$^{Cre/esr}$;*β-Cat*^{loxEx3} UE (arrowheads, B″). *Bmp4* is normally expressed in distal mesenchyme (C), is downregulated in *Shh*$^{Cre/esr}$;*β-Cat*$^{c/c}$ GT (C′), and is ectopically activated in the dUE of *Shh*$^{Cre/esr}$;*β-Cat*^{loxEx3} GT (C″, arrows). Note the complementary expression pattern of *Shh* and *Bmp4* in *Shh*$^{Cre/esr}$;*β-Cat*^{loxEx3} dUE (B″,C″). Scale bars: 100 μm.

ectodermal cover (Fig. 6P). Immunostaining of E12.5 mutant GT sagittal sections revealed that β-catenin-positive endodermal cells were not covered by β-catenin-negative ectodermal cells (see Fig. S4D, arrowheads, in the supplementary material). Consistently, *Shh*-expressing UE was exposed (Fig. 6Q,R). At E13.5, the mutant developed an open urethra, evidenced by histology, lineage-tracing and *Shh* expression (Fig. 6S-X). The defects were unlikely to be caused by a disruption in WNT signaling because TOPGAL-positive cells were still present in the urethral epithelium of *Msx2-Cre;β-Cat*$^{c/c}$ GT (Fig. S4F in the supplementary material). Moreover, the expression of *Tcf1* and *Fgf8* remained largely unchanged, except for a distal shift in expression domain; the shift was probably secondary to an overall structural change in these mutants (see Fig. S4H in the supplementary material, data not shown).

Conversely, cell-cell adhesion among ectodermal cells, and between ectodermal and endodermal cells, appeared to be compromised in the *Msx2-Cre;β-Cat*$^{c/c}$ mutants. Toluidine Blue-stained plastic sections and transmission electron microscopy (TEM) analyses revealed that the mutant ectoderm was much thinner than that of the control at E10.5 (Fig. 7A-D). At E12.5, nuclei of the ectodermal cells in the mutants were elongated, indicative of a stretched epithelium (Fig. 7G,H). Both plastic section and TEM showed that contact between the ectoderm and the endoderm was disrupted in the mutants (Fig. 7B,D, asterisks). Interestingly, the apparent deficit in epithelial integrity in the mutant occurred despite the seemingly normal distribution of α-catenin and E-cadherin at the cell membrane (data not shown, Fig. 7M,N). We also noted that plakoglobin expression was elevated in the ectoderm (Fig. 7L, arrows), which might partially compensate for the loss of β-catenin in adherens junctions. This upregulation was also confirmed by real-time PCR analysis (data not shown). To assess mutant epithelial differentiation, we examined the expression of p63 and K14. In E10.5 and E12.5 embryos, normal p63 expression was detected in the ventral ectoderm and the endodermal urethra of both wild-type and mutant GTs (data not shown, Fig. 7O,P). By contrast, K14 was not expressed in the genital ectoderm until E12.5 in wild-type GTs, and its expression was absent in the ventral ectoderm of mutant GTs (Fig. 7Q,R). This loss of K14 expression was not specific to the genital epithelium but was also observed in other regions of ectoderm where β-catenin was deleted (data not shown). Together, these results indicate that ectodermal β-catenin is required to maintain the integrity of the genital epithelium.

Role of mesenchymal β-catenin

Unlike the ecto- and endodermal Cre lines, mesenchymal *Dermo1-Cre* can only achieve patchy β-catenin deletion despite global recombination at the R26 locus in the GT mesenchyme (see Fig. S5H in the supplementary material). Nevertheless, SEM analysis showed that *Dermo1*-Cre; *β-Cat*$^{c/c}$ GTs were much smaller and were severely dysmorphic (Fig. S5B,D,F in the supplementary material). PHH3 staining demonstrated a reduction in cellular proliferation in the mutant mesenchyme (Fig. S5J,L in the supplementary material). Mitotic index was calculated in eight different mutants and seven wild types by counting PHH3-positive cells in a 0.03-mm^2 region. A more than twofold reduction was detected in the mutant (5.29±0.95% in controls versus 2.24±0.53% in mutants, P<0.0001). Consistently, mesenchymal expression of cyclin D1, a cell cycle regulator and a direct WNT target, was also downregulated (see Fig. S5N in the supplementary material). These results indicate a role for β-catenin in GT mesenchyme in promoting cell proliferation. However, activation of β-catenin by this Cre line resulted in early lethality, which prevented us from further analyzing its function in GT mesenchyme.

DISCUSSION

Most studies on genitalia development have focused on the role of androgen signaling, while much less is known about the genetic program governing early androgen-independent GT development. With the advent of Cre/LoxP technology, we have now investigated the function of β-catenin in GT development in a tissue-specific manner, and have demonstrated distinct functions for β-catenin in each tissue layer.

Our data showed that the timing of β-catenin removal from the endodermal urethra correlated with the severity of GT outgrowth defects. Deletion around GT initiation completely abrogated *Fgf8* induction in the dUE and subsequent GT outgrowth, whereas later removal resulted in reduced *Fgf8* expression and an underdeveloped GT. The graded GT phenotypes are similar to earlier findings in the limb, in which AER removal at successive time points caused limb truncations at increasingly distal positions (Saunders, 1948), supporting a conserved function of dUE and AER in directing appendage outgrowth (Cohn, 2004; Minelli, 2002; Yamada et al., 2006). Although it has long been recognized that the distal signaling centers are essential for appendage outgrowth, less is known about how they are initially established and restricted to a specific region within a seemingly homogeneous epithelium. Our data have demonstrated that the activation of WNT-β-catenin signaling is necessary and sufficient to activate *Fgf8* expression both in early cloacal endoderm and in later UE during GT development. Similarly, when we activated WNT-β-catenin signaling in the inter-limb ectoderm and non-AER limb ectoderm, *Fgf8* was ectopically expressed and, as a result, ectopic outgrowth was observed. These data demonstrated that, within a developmental window, the ectoderm and cloacal endoderm are competent to respond to activated WNT-β-catenin signaling and induce *Fgf8* expression. The fact that ectopic WNT-β-catenin signaling is sufficient to initiate *Fgf8* expression and outgrowth suggests that restricting WNT-β-catenin activity to a precise location represents a crucial step in determining the position and physical dimensions of the AER and dUE. Unfortunately, what mechanism restricts WNT-β-catenin activity to the signaling center remains largely unknown.

Epithelial-mesenchymal interactions play crucial roles during organogenesis (Hogan, 1999), including external genitalia development (Kurzrock et al., 1999b; Murakami and Mizuno, 1986). Once established, the dUE regulates mesenchymal gene expression and directs outgrowth. In this study, we identified a set of regulatory genes, including *Msx2*, *Lef1*, *Bmp4* and *Wnt5a*, whose expression depends on dUE signaling. These data provide in vivo evidence for the function of dUE in orchestrating and maintaining mesenchymal gene expression.

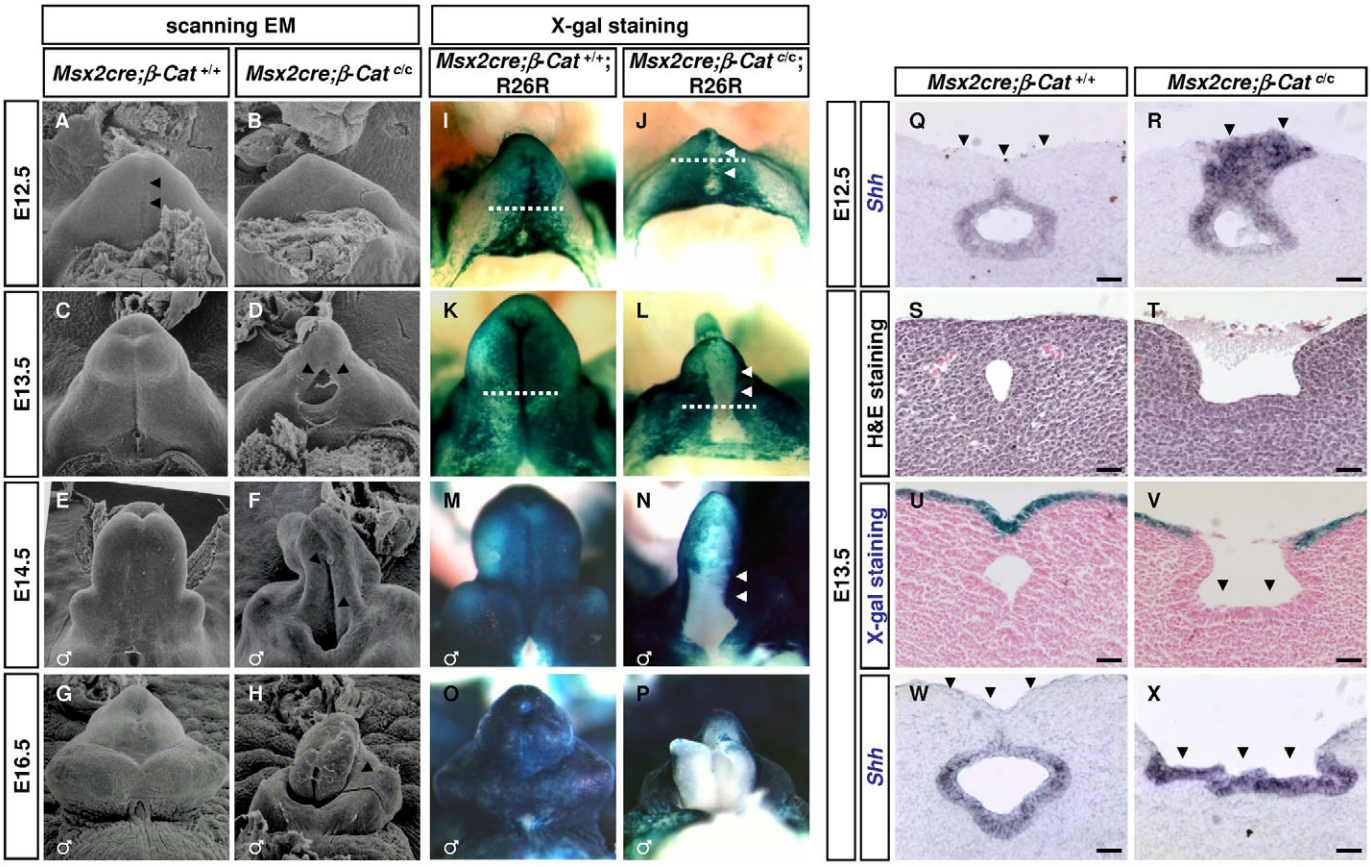

Fig. 6. Ectodermal defects in *Msx2-Cre;β-Cat*$^{c/c}$ GTs. (**A-H**) SEM analysis of wild-type and *Msx2-Cre;β-Cat*$^{c/c}$ GTs. *Msx2-Cre;β-Cat*$^{c/c}$ GTs show absence of an urethral seam (arrowheads, A) at E12.5 (B), an ectopic opening in proximal GT at E13.5 (arrowheads, D), and a distal bifurcation at E14.5 (arrowhead, F). (**I-P**) Tissue lineage analysis revealed an ectodermal rupture in *Msx2*-cre;*β-Cat*$^{c/c}$ GTs. The development of the ectodermal surface epithelium marked by *Msx2-Cre;R26R* was examined by X-Gal staining. β-Gal-positive ectodermal cells (blue) cover the entire GT surface throughout early development (I,K,M,O). By contrast, the mutant surface epithelium breaks down at the midline (arrowheads, J) and the disruption continues to expand (L,N). At E16.5, the ventral side of the GT is completely devoid of β-Gal-positive ectodermal epithelium (P). (**Q**,**R**) *Shh* in situ hybridization showing that *Shh*-expressing UE is covered by ventral ectoderm in wild-type GT (arrowheads, Q), but is exposed and expanded on the GT surface in *Msx2*-Cre;*β-Cat*$^{c/c}$ GTs at E12.5 (arrowheads, R). The planes of section are indicated in I,J. (**S**,**T**) H&E staining showing an ectopic opening in the proximal region of *Msx2*-Cre;*β-Cat*$^{c/c}$ GTs (T). (**U**,**V**) X-Gal staining showing that exposed epithelium in the mutant GT is *Msx2-Cre* negative. (**W**,**X**) *Shh* in situ hybridization showing that the exposed epithelium (arrowheads, X) expresses *Shh*. The planes of section in S-X are indicated in K and L. Scale bars: 100 μm in Q-X.

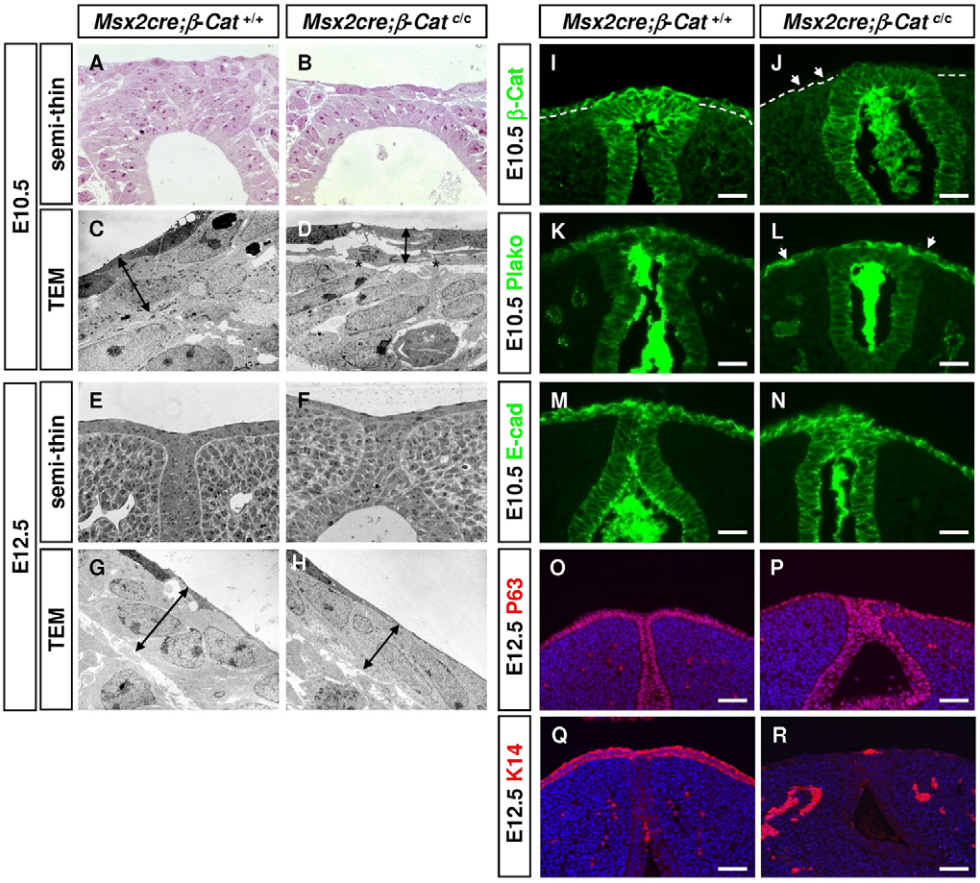

Fig. 7. Ectodermal structural defects in *Msx2-Cre;β-Cat*$^{c/c}$ embryos. (**A-H**) Toluidine Blue staining (A,B,E,F) and TEM analyses (C,D,G,H) on E10.5 coronal sections (A-D) and E12.5 transverse sections (E-H) reveal that the mutant surface epithelium is thinner (compare D to C, H to G). In addition, the ectoderm and endoderm maintain close contact in wild-type GTs (A,C), whereas the two layers appear to be separated in mutants (asterisks, D). (**I-N**) Immunostainings indicate an absence of β-catenin (J), an upregulation of plakoglobin (arrows, L) and normal E-cadherin expression in mutant ectoderm (N). (**O-R**) Immunostainings showing a total absence of K14 expression (R) but unchanged p63 expression (P) in E12.5 mutant ectoderm. Scale bars: 50 μm in I-N; 100 μm in O-R.

Our data also demonstrated a requirement for WNT-β-catenin signaling in the growth and patterning of endodermal urethra, as LOF mutant GTs showed an open urethra accompanied by reduced cellular proliferation. We specifically focused on analyzing the expression of two known important regulators of cell proliferation and apoptosis, *Shh* and *Bmp4* (Haraguchi et al., 2001; Perriton et al., 2002; Suzuki et al., 2003). The genetic hierarchy for *Wnt*, *Shh* and *Bmp4* has not been established in GT development. Our data suggest that *Bmp4* acts genetically downstream of WNT-β-catenin in dUE in a cell-autonomous manner and in GT mesenchyme in a non-cell-autonomous manner, possibly mediated by Fgf8, as the application of FGF*8*-soaked beads can stimulate *Bmp4* expression in GT mesenchyme (Haraguchi et al., 2000). Conversely, *Shh* can repress *Bmp4* expression in dUE, evidenced by the ectopic *Bmp4* induction in *Shh*$^{-/-}$ GT (Haraguchi et al., 2001). In our mutants, *Shh* downregulation also correlates with ectopic *Bmp4* activation in dUE, but only in the presence of WNT-β-catenin and FGF8 signaling. As *Fgf8* induction occurs in *Shh*$^{-/-}$ GT and *Shh* expression is downregulated in β-catenin LOF dUE, these data suggest that β-catenin is at the top of a genetic hierarchy regulating *Fgf8*, *Shh* and *Bmp4* expression (Fig. 8). However, we obtained an unexpected result in which *Shh* exhibited a bimodal response to activated WNT-β-catenin signaling in GOF mutants (Fig. 5B″). One possibility is that ectopic *Bmp4* expression in the distal urethral cells is responsible for *Shh* repression in this region. In support of this notion, *Bmp4* and *Shh* have been shown to repress the transcription of one another in other developmental systems (Monsoro-Burq and Le Douarin, 2001; Zhang et al., 2000). Alternatively, ectopic *Bmp4* expression might be secondary to *Shh* downregulation, and, in this case, it is not clear what mediates the bimodal response of *Shh*. Taken together, we propose a GT signaling pathway (summarized in Fig. 8) in which WNT-β-catenin signaling regulates both *Fgf8* and *Shh* expression, and *Shh* in turn inhibits *Bmp4*. Thus, it appears that the balance between the positive regulators of cell proliferation, *Fgf8* and *Shh*, and the negative regulator *Bmp4* controls cellular proliferation in the urethra to maintain homeostasis. In addition to *Fgf8* and *Shh*, *Fgfr2* is also required for urethral cell proliferation (Petiot et al., 2005). *Fgfr2* expression was visibly reduced in both β-catenin LOF and GOF urethrae (see Fig. S3E′,E″ in the supplementary material), as evidenced by in situ analysis, although real-time PCR confirmed such a reduction only in LOF UE. The urethra phenotype in the β-catenin LOF mutant was similar to that observed in *Fgfr2IIIb*$^{-/-}$ mutants (Petiot et al., 2005). However, unlike in *Fgfr2IIIb*$^{-/-}$ embryos, the expression of K14, a progenitor cell marker for squamous epithelium, was maintained. Thus, the defects observed in our LOF GT were unlikely to be caused by reduced FGFR2 signaling. The interaction between the WNT-β-catenin and FGFR2 signaling pathways needs further investigation.

Canonical WNT activity was not detected in the ventral ectoderm. Consistently, WNT signaling in the ectodermal β-catenin LOF GT does not seem to be affected, as evidenced by the presence of TOPGAL-positive cells and normal *Fgf8* and *Tcf1* expression. Nonetheless, the removal of ectodermal β-catenin still resulted in severe GT malformations. Tissue lineage analysis revealed an ectodermal breakdown at the ventral midline and subsequent urethral exposure, which implied that the ability of β-catenin$^{-/-}$ ectoderm to contain the growing GT was compromised. Consistently K14, an intermediate filament protein that gives tensile strength to epithelium, is not expressed in the mutant ectoderm, and the fact that mutant ectoderm shows signs of stretching suggest that

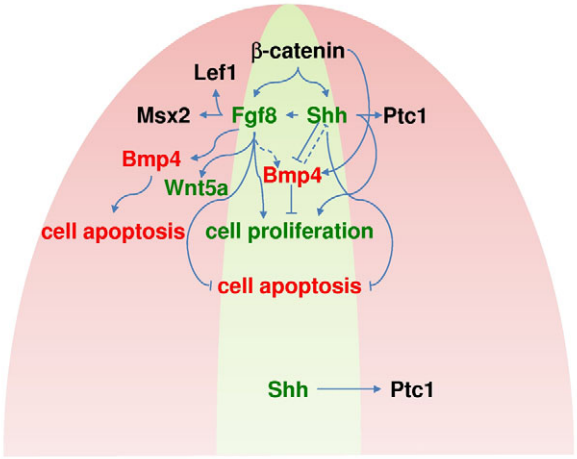

Fig. 8. A model of signaling crosstalks regulating GT development. Evidence indicates that canonical WNT acts upstream of *Fgf8* and *Shh* in the dUE. *Fgf8* expression in turn is required for establishing distal mesenchymal gene expression in the GT. *Shh* expression is also dependent on WNT activity. Shh normally represses *Bmp4* expression in the dUE. When WNT is constitutively activated, *Bmp4* is ectopically turned on in dUE. The coordinated regulation of positive (e.g. *Fgf8* and *Shh*, green) and negative (e.g. *Bmp4*, red) regulators of GT outgrowth is essential to maintain the homeostasis of the UE, as well as normal patterning of the GT. The pink region represents the distal mesenchyme; the green region represents the UE.

a lack of tensile support could directly contribute to the phenotype. In β-catenin-deficient ectoderm, we observed abnormal epithelial morphology and disrupted ectodermal-endodermal connection during initial GT outgrowth. Therefore, although we could not formally exclude disrupted WNT signaling as a cause of the mutant phenotype, it is more likely that weakened cell-cell adhesion was responsible for the ectodermal rupture. During early androgen-independent GT development, the endodermal urethra remains attached to the ventral surface epithelium (Perriton et al., 2002). As the GT protrudes from the ventral body wall, the ectoderm contacting the urethra would receive an increased physical force. A well-formed ectodermal-endodermal connection in this region may be required for structural support and to coordinate the growth of the two epithelia. This function for β-catenin in cell adhesion has also been implicated in other developmental systems (Cattelino et al., 2003; Fu et al., 2006). Why could overexpression of plakoglobin in the mutant GT ectoderm not compensate for the function of β-catenin in cell adhesion? We propose that although plakoglobin can connect E-cadherin to α-catenin and maintain the basic structure of adherens junctions, such a junction might not provide the same adhesive force as the wild-type congeners. In plakoglobin knockout mice, it is known that β-catenin can only partially compensate its function in desmosomes (Bierkamp et al., 1999). These results suggest that both plakoglobin and β-catenin have unique functions in cell adhesion that cannot be fully compensated.

In humans, hypospadias is defined as an abnormal urethral opening anywhere along the ventral side of the penis and scrotum. Both genetic and endocrine factors are implicated in the etiology of hypospadias. Androgen signaling is particularly important because hypospadias is commonly considered a male disease, although cleft clitoris does occur (Baskin and Ebbers, 2006). Both our endodermal and ectodermal β-catenin conditional-knockout mice exhibited a severe hypospadias phenotype in both sexes. These results raise the possibility that the disruption of WNT-β-catenin signaling and/or proper cell adhesion by either somatic mutation or endocrine disruption during GT development may lead to external genital abnormalities, including hypospadias in humans. Future research on genetic mechanisms and endocrine-genetic interaction could shed light on external genitalia development, as well as on the pathogenesis of hypospadias and other congenital malformations.

We thank Drs Yongjun Yin and David Ornitz for sharing *Dermo1-Cre;β-Cat$^{c/c}$* mice and for their invaluable comments on the manuscript. We also thank Dr David Beebe for Phospho-Smad antibody, Mike Veith for help on electron microscopy, Dr Gen Yamada for exchanging progress before publication and Dr Raphael Kopan for critical reading of the manuscript. This work was supported by National Institutes of Health Grants HD41492 and ES014482.

Supplementary material

Supplementary material for this article is available at http://dev.biologists.org/cgi/content/full/135/16/2815/DC1

References

Barrow, J. R., Thomas, K. R., Boussadia-Zahui, O., Moore, R., Kemler, R., Capecchi, M. R. and McMahon, A. P. (2003). Ectodermal Wnt3/beta-catenin signaling is required for the establishment and maintenance of the apical ectodermal ridge. *Genes Dev.* **17**, 394-409.

Baskin, L. S. and Ebbers, M. B. (2006). Hypospadias: anatomy, etiology, and technique. *J. Pediatr. Surg.* **41**, 463-472.

Baskin, L. S., Erol, A., Jegatheesan, P., Li, Y., Liu, W. and Cunha, G. R. (2001). Urethral seam formation and hypospadias. *Cell Tissue Res.* **305**, 379-387.

Bierkamp, C., Schwarz, H., Huber, O. and Kemler, R. (1999). Desmosomal localization of beta-catenin in the skin of plakoglobin null-mutant mice. *Development* **126**, 371-381.

Bitgood, M. J. and McMahon, A. P. (1995). Hedgehog and Bmp genes are coexpressed at many diverse sites of cell-cell interaction in the mouse embryo. *Dev. Biol.* **172**, 126-138.

Brault, V., Moore, R., Kutsch, S., Ishibashi, M., Rowitch, D. H., McMahon, A. P., Sommer, L., Boussadia, O. and Kemler, R. (2001). Inactivation of the beta-catenin gene by Wnt1-Cre-mediated deletion results in dramatic brain malformation and failure of craniofacial development. *Development* **128**, 1253-1264.

Cattelino, A., Liebner, S., Gallini, R., Zanetti, A., Balconi, G., Corsi, A., Bianco, P., Wolburg, H., Moore, R., Oreda, B. et al. (2003). The conditional inactivation of the beta-catenin gene in endothelial cells causes a defective vascular pattern and increased vascular fragility. *J. Cell Biol.* **162**, 1111-1122.

Cohn, M. J. (2004). Developmental genetics of the external genitalia. *Adv. Exp. Med. Biol.* **545**, 149-157.

Cohn, M. J., Izpisua-Belmonte, J. C., Abud, H., Heath, J. K. and Tickle, C. (1995). Fibroblast growth factors induce additional limb development from the flank of chick embryos. *Cell* **80**, 739-746.

Crossley, P. H. and Martin, G. R. (1995). The mouse Fgf8 gene encodes a family of polypeptides and is expressed in regions that direct outgrowth and patterning in the developing embryo. *Development* **121**, 439-451.

Crossley, P. H., Minowada, G., MacArthur, C. A. and Martin, G. R. (1996). Roles for FGF8 in the induction, initiation, and maintenance of chick limb development. *Cell* **84**, 127-136.

DasGupta, R. and Fuchs, E. (1999). Multiple roles for activated LEF/TCF transcription complexes during hair follicle development and differentiation. *Development* **126**, 4557-4568.

Dolle, P., Dierich, A., LeMeur, M., Schimmang, T., Schuhbaur, B., Chambon, P. and Duboule, D. (1993). Disruption of the Hoxd-13 gene induces localized heterochrony leading to mice with neotenic limbs. *Cell* **75**, 431-441.

Dudley, A. T., Ros, M. A. and Tabin, C. J. (2002). A re-examination of proximodistal patterning during vertebrate limb development. *Nature* **418**, 539-544.

Dunn, N. R., Winnier, G. E., Hargett, L. K., Schrick, J. J., Fogo, A. B. and Hogan, B. L. (1997). Haploinsufficient phenotypes in Bmp4 heterozygous null mice and modification by mutations in Gli3 and Alx4. *Dev. Biol.* **188**, 235-247.

Felix, W. (1912). The development of the urogenital organs. In *Manual of Human Embryology* (ed. F. P. Mall), pp. 752-973. Philadelphia: J. B. Lippencott Company.

Fromental-Ramain, C., Warot, X., Messadecq, N., LeMeur, M., Dolle, P. and Chambon, P. (1996). Hoxa-13 and Hoxd-13 play a crucial role in the patterning of the limb autopod. *Development* **122**, 2997-3011.

Fu, X., Sun, H., Klein, W. H. and Mu, X. (2006). Beta-catenin is essential for lamination but not neurogenesis in mouse retinal development. *Dev Biol.* **299**, 424-437.

Gregorieff, A., Grosschedl, R. and Clevers, H. (2004). Hindgut defects and transformation of the gastro-intestinal tract in Tcf4(–/–)/Tcf1(–/–) embryos. *EMBO J.* **23**, 1825-1833.

Harada, N., Tamai, Y., Ishikawa, T., Sauer, B., Takaku, K., Oshima, M. and Taketo, M. M. (1999). Intestinal polyposis in mice with a dominant stable mutation of the beta-catenin gene. *EMBO J.* **18**, 5931-5942.
Haraguchi, R., Suzuki, K., Murakami, R., Sakai, M., Kamikawa, M., Kengaku, M., Sekine, K., Kawano, H., Kato, S., Ueno, N. et al. (2000). Molecular analysis of external genitalia formation: the role of fibroblast growth factor (Fgf) genes during genital tubercle formation. *Development* **127**, 2471-2479.
Haraguchi, R., Mo, R., Hui, C., Motoyama, J., Makino, S., Shiroishi, T., Gaffield, W. and Yamada, G. (2001). Unique functions of Sonic hedgehog signaling during external genitalia development. *Development* **128**, 4241-4250.
Harfe, B. D., Scherz, P. J., Nissim, S., Tian, H., McMahon, A. P. and Tabin, C. J. (2004). Evidence for an expansion-based temporal Shh gradient in specifying vertebrate digit identities. *Cell* **118**, 517-528.
Hogan, B. L. (1999). Morphogenesis. *Cell* **96**, 225-233.
Hu, H., Hilton, M. J., Tu, X., Yu, K., Ornitz, D. M. and Long, F. (2005). Sequential roles of Hedgehog and Wnt signaling in osteoblast development. *Development* **132**, 49-60.
Huang, W. W., Yin, Y., Bi, Q., Chiang, T. C., Garner, N., Vuoristo, J., McLachlan, J. A. and Ma, L. (2005). Developmental diethylstilbestrol exposure alters genetic pathways of uterine cytodifferentiation. *Mol. Endocrinol.* **19**, 669-682.
Jones, C. M., Lyons, K. M. and Hogan, B. L. (1991). Involvement of Bone Morphogenetic Protein-4 (BMP-4) and Vgr-1 in morphogenesis and neurogenesis in the mouse. *Development* **111**, 531-542.
Kurzrock, E. A., Baskin, L. S. and Cunha, G. R. (1999a). Ontogeny of the male urethra: theory of endodermal differentiation. *Differentiation* **64**, 115-122.
Kurzrock, E. A., Baskin, L. S., Li, Y. and Cunha, G. R. (1999b). Epithelial-mesenchymal interactions in development of the mouse fetal genital tubercle. *Cells Tissues Organs* **164**, 125-130.
Lewandoski, M., Sun, X. and Martin, G. R. (2000). Fgf8 signalling from the AER is essential for normal limb development. *Nat. Genet.* **26**, 460-463.
Mariani, F. V. and Martin, G. R. (2003). Deciphering skeletal patterning: clues from the limb. *Nature* **423**, 319-325.
Minelli, A. (2002). Homology, limbs, and genitalia. *Evol. Dev.* **4**, 127-132.
Monsoro-Burq, A. and Le Douarin, N. M. (2001). BMP4 plays a key role in left-right patterning in chick embryos by maintaining Sonic Hedgehog asymmetry. *Mol. Cell* **7**, 789-799.
Morgan, E. A., Nguyen, S. B., Scott, V. and Stadler, H. S. (2003). Loss of Bmp7 and Fgf8 signaling in Hoxa13-mutant mice causes hypospadia. *Development* **130**, 3095-3109.
Murakami, R. and Mizuno, T. (1986). Proximal-distal sequence of development of the skeletal tissues in the penis of rat and the inductive effect of epithelium. *J. Embryol. Exp. Morphol.* **92**, 133-143.
Niswander, L., Tickle, C., Vogel, A., Booth, I. and Martin, G. R. (1993). FGF-4 replaces the apical ectodermal ridge and directs outgrowth and patterning of the limb. *Cell* **75**, 579-587.
Perriton, C. L., Powles, N., Chiang, C., Maconochie, M. K. and Cohn, M. J. (2002). Sonic hedgehog signaling from the urethral epithelium controls external genital development. *Dev. Biol.* **247**, 26-46.
Petiot, A., Perriton, C. L., Dickson, C. and Cohn, M. J. (2005). Development of the mammalian urethra is controlled by Fgfr2-IIIb. *Development* **132**, 2441-2450.
Saunders, J. (1948). The proximo-distal sequence of origin of the parts of the chick wing and the role of the ectoderm. *J. Exp. Zool.* **108**, 363-403.
Scott, V., Morgan, E. A. and Stadler, H. S. (2005). Genitourinary functions of Hoxa13 and Hoxd13. *J. Biochem.* **137**, 671-676.
Soriano, P. (1999). Generalized lacZ expression with the ROSA26 Cre reporter strain. *Nat. Genet.* **21**, 70-71.
Spaulding, M. H. (1921). The development of external genitalia in the human embryo. *Carnegie Contrib. Embryol.* **61**, 67-88.
Summerbell, D. (1974). A quantitative analysis of the effect of excision of the AER from the chick limb-bud. *J. Embryol. Exp. Morphol.* **32**, 651-660.
Suzuki, K., Ogino, Y., Murakami, R., Satoh, Y., Bachiller, D. and Yamada, G. (2002). Embryonic development of mouse external genitalia: insights into a unique mode of organogenesis. *Evol. Dev.* **4**, 133-141.
Suzuki, K., Bachiller, D., Chen, Y. P., Kamikawa, M., Ogi, H., Haraguchi, R., Ogino, Y., Minami, Y., Mishina, Y., Ahn, K. et al. (2003). Regulation of outgrowth and apoptosis for the terminal appendage: external genitalia development by concerted actions of BMP signaling [corrected]. *Development* **130**, 6209-6220.
Tu, X., Joeng, K. S., Nakayama, K. I., Nakayama, K., Rajagopal, J., Carroll, T. J., McMahon, A. P. and Long, F. (2007). Noncanonical Wnt signaling through G protein-linked PKCdelta activation promotes bone formation. *Dev. Cell* **12**, 113-127.
Warot, X., Fromental-Ramain, C., Fraulob, V., Chambon, P. and Dolle, P. (1997). Gene dosage-dependent effects of the Hoxa-13 and Hoxd-13 mutations on morphogenesis of the terminal parts of the digestive and urogenital tracts. *Development* **124**, 4781-4791.
Wawersik, S. and Epstein, J. A. (2000). Gene expression analysis by in situ hybridization. Radioactive probes. *Methods Mol. Biol.* **137**, 87-96.
Wilkinson, D. G. (1992). *In Situ Hybridization: A Practical Approach*. London: Oxford University Press.
Yamada, G., Satoh, Y., Baskin, L. S. and Cunha, G. R. (2003). Cellular and molecular mechanisms of development of the external genitalia. *Differentiation* **71**, 445-460.
Yamada, G., Suzuki, K., Haraguchi, R., Miyagawa, S., Satoh, Y., Kamimura, M., Nakagata, N., Kataoka, H., Kuroiwa, A. and Chen, Y. (2006). Molecular genetic cascades for external genitalia formation: an emerging organogenesis program. *Dev. Dyn.* **235**, 1738-1752.
Yamaguchi, T. P., Bradley, A., McMahon, A. P. and Jones, S. (1999). A Wnt5a pathway underlies outgrowth of multiple structures in the vertebrate embryo. *Development* **126**, 1211-1223.
Yin, Y., Lin, C. and Ma, L. (2006). MSX2 promotes vaginal epithelial differentiation and wolffian duct regression and dampens the vaginal response to diethylstilbestrol. *Mol. Endocrinol.* **20**, 1535-1546.
Yu, K., Xu, J., Liu, Z., Sosic, D., Shao, J., Olson, E. N., Towler, D. A. and Ornitz, D. M. (2003). Conditional inactivation of FGF receptor 2 reveals an essential role for FGF signaling in the regulation of osteoblast function and bone growth. *Development* **130**, 3063-3074.
Zakany, J., Fromental-Ramain, C., Warot, X. and Duboule, D. (1997). Regulation of number and size of digits by posterior Hox genes: a dose-dependent mechanism with potential evolutionary implications. *Proc. Natl. Acad. Sci. USA* **94**, 13695-13700.
Zhang, Y., Zhang, Z., Zhao, X., Yu, X., Hu, Y., Geronimo, B., Fromm, S. H. and Chen, Y. P. (2000). A new function of BMP4: dual role for BMP4 in regulation of Sonic hedgehog expression in the mouse tooth germ. *Development* **127**, 1431-1443.